Adhesion of Lactobacillus rhamnosus GG surface biomolecules to milk proteins

Justine Guerin, Jennifer Burgain, Gregory Francius, Sofiane El-Kirat-Chatel, Audrey Beaussart, Joël Scher, Claire Gaiani

Adhesion of *Lactobacillus rhamnosus* GG surface biomolecules to milk proteins

Justine Guerin[a], Jennifer Burgain[a], Gregory Francius[b], Sofiane El-Kirat-Chatel[b], Audrey Beaussart[c], Joël Scher[a], Claire Gaiani[a]

[a]Université de Lorraine, LIBio, F-54000 Nancy, France

[b]CNRS, Université de Lorraine, LCPME, Laboratoire de Chimie Physique et Microbiologie pour l'Environnement, UMR 7564, 54600 Villers-lès-Nancy, France

[c]CNRS, Université de Lorraine, LIEC (Laboratoire Interdisciplinaire des Environnements Continentaux), UMR7360, Vandoeuvre-lès-Nancy F-54501, France.

*Corresponding author:

claire.gaiani@univ-lorraine.fr

Fax: +33 3 83 59 57 72.

Keywords

Milk proteins; *Lactobacillus rhamnosus* GG; Bacterial surface biomolecules; Pili; Adhesion; Atomic force microscopy

Abstract

Lactic Acid Bacteria (LAB) are not homogeneously located in the dairy matrix and their spatial distribution seems to be controlled by the establishment of adhesive interactions between matrix components and bacterial surface biomolecules. However the mechanisms of interaction remain unknown although they constitute an interesting way of study to appreciate the interactions. The aim of this work was to understand the role of surface biomolecules in the adhesion of *Lactobacillus rhamnosus* GG - the most used LAB strain in food products for their health benefits to the consumer - to milk proteins. Adhesions were probed using atomic force microscopy based force spectroscopy. To this end, the wild type strain and three of its surface mutants were employed. The wild type strain interacts with the β-lactoglobulin through the pili SpaCBA. The use of LGG surface mutants revealed that other surface biomolecules as long / small exopolysaccharides and proteins are involved in adhesion with milk proteins, in a less pronounced way than pili and in absence of pili, as all other surface biomolecules are masked in presence of pili. Altogether, this study demonstrates that adhesive interactions between LGG and milk proteins are governed by the surface composition of the bacteria.

1. Introduction

Lactic acid bacteria (LAB) are incorporated in many dairy products due to their fermentative properties and their probiotic characteristics. LAB are the most important starter cultures used in all area of dairy and food fermentation (Leroy & De Vuyst, 2004). By causing a rapid acidification of the raw material through the conversion of lactose into lactic acid, LAB play a central role in fermentation processes. LAB also produce several compounds (as acetic acid, ethanol, aromatic

compounds, bacteriocins, exopolysaccharides or enzymes) often involved in biochemical reactions during food processing which influence its texture and flavor. This is particularly the case during cheese ripening (Hickey, Sheehan, Wilkinson, & Auty, 2015; Leroy & De Vuyst, 2004). Many LAB are also incorporated into food products for their health benefits to the consumer. The strains *Lactobacillus rhamnosus* GG (LGG) (Valio), *Lactobacillus paracasei* Shirota (Yakult) or *Bifidobacterium lactis* BB12 (Chr. Hansen) are the most documented LAB used in food industries (Linares, Ross, & Stanton, 2016). Among these strains, LGG is also an interesting LAB model in food research because of its wide use, its available genome sequence (Kankainen et al., 2009) and the availability of numerous surface mutants (Lebeer et al., 2012). The surface composition of LGG is well-known and contains numerous SpaCBA pili distributed all around the bacterial cells (Reunanen, von Ossowski, Hendrickx, Palva, & de Vos, 2012; Tripathi et al., 2012), long galactose-rich exopolysaccharides (EPS), small glucose-rich EPS (Francius et al., 2009) and other proteins as MBF (von Ossowski et al., 2011) or MabA (Perea Vélez et al., 2010).

The spatial distribution of LAB within the dairy matrix plays an essential role during cheese processing, ripening and storage. This parameter may affect enzymes release and solutes diffusion in the matrix, which would influences cheese texture, flavor and aroma development (Hickey, Auty, Wilkinson, & Sheehan, 2015; Hickey et al., 2015). Numerous studies reported that LAB are not evenly distributed in the dairy matrix. During cheese ripening, various microscopy methods reported the preferential bacterial location at the fat-protein interface or in direct contact with the milk fat globule membrane (Laloy, Vuillemard, El Soda, & Simard, 1996; Lopez, Maillard, Briard-Bion, Camier, & Hannon, 2006; Oberg, McManus, & McMahon, 1993; Tunick et al., 1993). Previously published work from the authors demonstrated that bacteria surface biomolecules can play a key role in bacteria distribution within the food matrix. The presence of the SpaCBA pili, a

proteinaceous surface appendages, at the LGG surface leads to a homogeneous location of the bacteria in the matrix. In absence of pili on their surface, LGG bacteria are closely spaced and aggregated at the same place in the matrix (**Figure S1**). Therefore, bacteria location in the dairy matrix seems to be governed both by the matrix composition and the surface composition of the bacteria.

Deciphering adhesive interactions between LAB surface biomolecules and dairy compounds would allow to better understand -and eventually predict- bacteria location in a food product. Nevertheless, very few studies focused on this concern. In a recent work, atomic force microscopy (AFM) was used to reveal specific adhesive interactions between LGG and whey proteins (J. Burgain et al., 2013), and more particularly with the β-lactoglobulin (β-LG) (Guerin et al., 2016). Different LGG surface mutants were compared to understand the mechanism occurring during adhesive interactions and the key role of the SpaCBA pili was underlined (Burgain et al., 2013; Guerin et al., 2016). However, the role of the other surface biomolecules remains, to the best of our knowledge, unknown.

The aim of this study was to decipher, at the nanoscale, the interactions involved in the adhesion of LGG to different pure milk proteins: micellar caseins, β-LG, α-lactalbumin (α-LA) and bovine serum albumin (BSA). By comparing the adhesive forces of various LGG cell-wall mutants with these proteins, the role of different LGG surface biomolecules in the binding mechanisms was interpreted.

2. Material and methods

2.1 Material

Micellar caseins (Promilk 872B) are obtained from Ingredia IDI (Arras, France). The β-LG, α-LA and BSA are purchased from Sigma-Aldrich (France).

L. rhamnosus GG (ATCC 53103) (LGG WT) and three of its surface mutants are used. The surface mutants are: the pilus *spaCBA* knockout mutant CMPG5357 (LGG *spaCBA*) (Lebeer et al., 2012), the *welE* knockout EPS-deficient mutant CMPG5351 (LGG *welE*) (Lebeer et al., 2009; Lebeer, Claes, Verhoeven, Vanderleyden, & De Keersmaecker, 2011), the double knockout of the *spaCBA* operon and the *welE* gene CMPG5365 (LGG *welEspaCBA*) (Lebeer et al., 2012).

2.2 Microbial Adhesion To Solvent (MATS)

The four strains of LGG are cultivated as described by Guerin et al. (2016). Briefly, the growth of the four strains is performed at 37 °C in MRS broth until an optical density at 600 nm around 1.2 is reached. The culture is centrifuged at 3,000 g for 10 min at room temperature. The pellet is washed with PBS and re-suspended in PBS to obtain an optical density of 0.5 at 600 nm. The ability of LGG cell surface to adhere to solvent was evaluated as described by Salotti de Souza et al. (2018), with some modifications. For this determination, 1.2 ml of bacterial suspension in PBS is mixed for 90 s with 0.2 ml of different solvents. The bacterial affinity to a polar solvent (chloroform) and an apolar solvent (hexadecane) is studied. The mixtures are allowed to stand for 15 min to ensure the good separation of the two phases. Then, the optical density of the aqueous phase is measured at 600 nm. The percentage of bound cells is calculated with:

$$\%\, adhesion = \frac{A_0 - A}{A_0} \times 100$$

Where A_0 is the absorbance of the bacteria suspension measured at 600 nm before mixing and A is the absorbance of the bacteria suspension measured at 600 nm after mixing.

2.3 Atomic force microscopy

2.3.1 Preparation of bacteria-coated mica

A mica coated with a gold layer functionalized with a NH_2 terminated PEG linker (Novascan, Ames, Iowa, USA) is used in this study. Culture of LGG is performed as describe by Guerin *et al.* (Guerin et al., 2016). The bacterial suspension is deposed on mica during 15 h at 4 °C (pH 6.8). The mica is rinsed with PBS (pH 6.8) before their use. AFM topographic images confirmed the presence and the good coverage of LGG on the mica surface (**Figure S2**).

2.3.2 Preparation of proteins-coated tips

AFM probes with borosilicate glass particle (2 µm), coated with gold and modified with NH_2 terminated PEG linker are used (Novascan, Ames, Iowa, USA). The nominal spring constant is 0.01 N/m. Milk proteins (micellar caseins, β-LG, α-LA, BSA) are prepared in distilled water at a concentration of 1 % (w/w). The rehydration is done under stirring for 2 h at room temperature and overnight at 4 °C. Proteins are adsorbed on the probe by immersion for 15 h at 4 °C. The time left for adsorption is much higher than time necessary for the proteins to absorb on the tip. Probes are rinsed with milli-Q-grade water before use.

2.3.3 Atomic force microscopy measurements

Force measurements are performed at room temperature in PBS buffer (pH 6.8) using an Asylum MFP-3D atomic force microscope (Santa Barbara, CA, USA) controlled by the operation software IGOR Pro 6.04 (Wavemetrics, Lake Osewego, OR, USA) as described by Guerin *et al.* (2016). The tip coating can slightly modify the cantilever spring constant but the modification is taken into account by readjusting the value *via* the thermal noise method. For each experiment, the force map

is obtained on a 10 × 10 µm² surface corresponding to 32 × 32 points, *i.e.* 1024 force curves. AFM force distance curves are obtained by following the cantilever deflection as a function of the vertical displacement of the piezoelectric scanner with a scan speed of 400 mm/s.

2.3.4 Curve processing

Determination of the percentage of adhesive events. For each AFM force measurement, a force map containing 1024 force curves is recorded. The presence of specific adhesion between bacteria and milk proteins are determined by analyzing the retraction curves. The force profiles often show multipeaks, corresponding to the stretching of biomolecules. For each experiment, 100 force curves are selected and the corresponding retraction curves are considered to determine the percentage of adhesive events with specific biomolecule stretching signatures.

Retraction curves analysis. All retraction curves presenting specific biomolecule stretching signatures are fitted with two predictive models: FJC (Freely-Jointed Chain) model and WLC (Worm-Like Chain) model. These two models are used to describe the elongation by statistical mechanics of ideal chains (Guerin et al., 2016). These predictive models permit to access parameters such as: number of rupture, maximal rupture force needed to detach the biomolecule, the maximum extension length of the biomolecule before rupture and the contour length of the biomolecule. The maximal adhesion force needed to break the contact between bacteria and milk proteins is calculated through the analysis of the retraction curve. All the information are illustrated in **Figure 1**.

SpaCBA pili mechanical behavior. To quantify the mechanical behavior of SpaCBA pili, spring constant in different loading regimes is estimated as described by Tripathi *et al. (2013)*. The pili

spring constant (k_p) is determined using the slope (s) of the linear portion of the curve and the following equation:

$$k_p = (k_c \times s) \div (1 - s)$$

with k_c (pN/µm) the spring constant of AFM cantilever. The constant force step values (F_p, pN) and the constant length values (L_p, nm) are determined by measuring the force and the length of the constant force plateaus on the retraction curve.

3. Results and Discussion

Bacterial surface characterization

To better clarify and explain the adhesive interactions occurring between bacteria and milk proteins, surface properties of the different LGG mutant strains were investigated. Bacterial surface charge and hydrophobicity may be very important to explain the nature of the interactions. In this study, adhesion force measurements are performed in PBS. PBS possesses a high molarity sufficient to mask the charges of both LGG surface and proteins (Burgain et al., 2015). Therefore, the charge of bacteria should not influence the adhesive interactions with proteins. On the contrary, the surface hydrophobicity of the four different strains seems important to better highlight the nature of the interactions between bacteria and milk proteins. With the MATS method, LGG WT, LGG *welE* and LGG *welEspaCBA* showed a more hydrophilic surface character with a best affinity to chloroform compared to hexadecane. On the contrary, LGG *SpaCBA* presented a more hydrophobic surface character with a poorer affinity to chloroform (**Figure 2**).

Key role of SpaCBA pili in milk proteins adhesion

Some of the biomolecules present at the surface of LGG WT comprise the SpaCBA pili, the long galactose-rich EPS, the small glucose-rich EPS and other proteins as MBF (Mucus Binding Factor) or MabA (**Figure 3A**). AFM-based force spectroscopy is used with milk proteins coated probes to decipher how LGG WT cells interact with these individual proteins. The percentage of adhesive events presented in **Figure 3B** reveals major differences between the four milk proteins tested.

The percentage of specific adhesive events is of 66.5 ± 0.5, 3.5 ± 1.5 and 9.0 ± 0.0 % for β-LG, α-LA and BSA, respectively. No adhesive event is observed with caseins. The percentage of adhesive events is very high for β-LG. The force signatures observed with β-LG are very repeatable and correspond to specific events (**Figure 3C**). For α-LA and BSA, the percentage of adhesive events is very low (**Figure 3B**). The force signatures corresponding to these low adhesive interactions with α-LA and BSA (**Figures 3E and 3F**) are poorly repeatable which suggest that they are unspecific events.

The specific adhesion between LGG WT and β-LG reinforces previous hypothesis suggested by Guerin *et al.* (2016) who proposed that the adhesion between LGG WT and β-LG is mediated by SpaCBA pili. To support this result, the retraction curves recorded between these two entities are analyzed in details (**Figure 3C and 3D**). Remarkable adhesion signatures are detected on retraction curves between LGG WT and β-LG. Large adhesion force peaks with linear shape and characteristic horizontal force steps are observed (**Figure 3C**). These adhesion signatures are comparable to those observed by Tripathi *et al.* (2013), who demonstrate, using AFM tips decorated with SpaC proteins to pull on pili at the surface of LGG cells, that the appendages behave like a nanospring under mechanical stretching. Superimposition of multiple forces profiles reveals

a high reproducibility of the events (**Figure 3D**). As described by Tripathi *et al.* (2013), the specific signatures repetition are most-likely due to the intrinsic mechanical properties of SpaCBA pili. The different linear slopes and plateau values observed on the 'step curves' were then analyzed. The slopes of the linear segments are found to increase with increasing the applied pulling force. This behavior describes the stiffening of the stretched pilus. The spring constant of pili (k_p) in the different loading rate is then calculated and found to be k_{p1} = 5.6 ± 1.0, k_{p2} = 11.7 ± 0.8 and k_{p3} = 19.1 ± 1.1 pN/µm. Besides, the constant force steps values (F_{p1} = 129 ± 8 and F_{p2} = 310 ± 8 pN) and the constant step length values (L_{p1} = 91 ± 6 and L_{p2} = 109 ± 10 nm) are highly reproducible. The values variation follow the same trend that those measured by Tripathi *et al.* (2013) and Sullan *et al.* (2014). These characteristics are reproducible and confirm the structural changes of the SpaCBA pilus induced during the retraction of the β-LG tip, leading to a more rigid conformation of the pilus. These results demonstrated the nanospring-like behavior of pilus SpaCBA during adhesion with the β-LG.

Caseins and whey proteins structures differ. Caseins are organized in spherical and voluminous superstructures called micelles and present a lack of secondary organization (Fox, 2008). On the contrary, whey proteins (including β-LG) possess a rich secondary organization with β-sheet and α-helix structures and the presence of disulfide bonds. Contrary to α-LA and BSA, β-LG monomers are folded into eight stranded antiparallel β-sheets that form a hydrophobic pocket, called calix, with a 3-turn -helix on the outer surface (Monaco et al., 1987), able to bind multiple hydrophobic molecules (Çelebioğlu et al., 2015; Dominguez-Ramirez, Del Moral-Ramirez, Cortes-Hernandez, Garcia-Garibay, & Jimenez-Guzman, 2013; Kontopidis, Holt, & Sawyer, 2002, 2004). The difference observed in the percentage of adhesive events between LGG WT and the proteins may be due to a difference of structure. It worth consider that LGG WT interact preferentially with

β-LG due to the presence of a hydrophobic calix. However the calix is probably not able to interact with a larger molecule such as the LGG pili SpaCBA protein. Moreover the SpaCBA pili is a glycosylated proteins (Tytgat et al., 2016), so the interaction between LGG WT and the β-LG would be more hydrophilic rather than hydrophobic. MATS method confirms the hydrophilic character of the LGG WT surface (**Figure 2**). Therefore, the hydrophilic nature of the interaction occurring between the LGG WT and the β-LG is confirmed.

To confirm the role of SpaCBA pili in adhesion to β-LG, the LGG *welE* strain, deprived of long rich-galactose EPS layer, is used. This mutant is known to overexpose SpaCBA pili, due to the EPS removal (**Figure 4A**) (Lebeer et al., 2012). The percentages of adhesive events between LGG *welE* and β-LG (96.5 ± 1.5 %) are higher than LGG WT (66.5 ± 0.5 %) (**Figure 4B**). In LGG *welE*, pili located on bacterial surface are not embedded within the EPS layer and are entirely free to establish contact points with β-LG. A recent work has demonstrated the glycosylated behavior of the stretched biomolecule during interaction between β-LG and LGG WT and LGG *welE* (Guerin et al., 2016). It appears that the SpaC pilins of the SpaCBA pili are the pilins carrying the glycosylation (Tytgat et al., 2016), suggesting that SpaC subunits is implicated in β-LG interaction. In LGG *welE*, the increased exposure of SpaC pilins at the basal part of each pilus could allow SpaCBA pili to establish more contact points with β-LG resulting in an increased number of rupture events in the retraction curve (Lebeer et al., 2012). The specific biomolecules stretching signatures between β-LG and LGG *welE* differed from LGG WT with the apparition of more irregular and jerky signatures and a more important maximal rupture distance (2.8 ± 0.5 and 1.1 ± 0.1 µm for LGG *welE* and LGG WT, respectively) (**Figure 4C**). As the size of a SpaCBA pilus is around 1 µm (Guerin et al., 2016; Tripathi et al., 2013), the biomolecule stretched at a distance of around 2.8 µm with LGG *welE* might not be an individual pilus. In fact, the pilus SpaCBA is able to

interact each other with a zipper-like adhesion mechanism involving multiple SpaC molecules distributed along the pilus length. In LGG *welE*, SpaCBA pili are not embedded in EPS layer and are totally free to interact with each other. SpaCBA pili may form a network entirely engaged in the interaction and leading to the observed numerous ruptures and the presence of jerky signatures during the retraction of the tip containing β-LG which leads to a stretched distance of 2.8 µm with LGG *welE*.

Surprisingly, a lot of adhesive events are observed between LGG *welE* and other milk proteins (caseins, α-LA and BSA). The percentages of adhesive events are of 56.0 ± 6.5, 98.5 ± 1.5 and 88.5 ± 2.5 % for caseins, α-LA and BSA, respectively (**Figure 4B**). It was previously shown that these three proteins poorly interact with LGG WT. In contrast, a lot of specific signatures, similar to those observed with β-LG, are observed with LGG *welE* (**Figure 3C, E and F**). In LGG *welE*, the over-exposition of the SpaCBA pili in absence of long EPS layer could allowed caseins, α-LA and BSA to interact with SpaCBA pili. An explanation would be that, for LGG *welE*, the absence of long EPS lead to uncover pili subunits initially buried in the EPS structure. It can be the case of the SpaB pilins, which are located at the pilus base. In the absence of long-EPS layer, these SpaB subunits would be accessible to promote interaction between LGG *welE* and these three milk proteins. To verify this hypothesis, adhesion force measurements should be made between milk proteins and purified SpaCBA pili or purified subunits SpaB of the pilus. The rupture distance observed on retraction curve was too long to believe that other surface biomolecules such as MabA and MBF proteins or small EPS governed interaction between LGG *welE* and milk proteins.

In conclusion, the SpaCBA pili environment seems to determine LGG ability to interact with milk proteins. In presence of long-EPS layer, the SpaCBA pili interact preferably with β-LG. In absence of long-EPS layer, SpaCBA pili possess the ability to adhere with all the studied milk proteins.

Role of EPS and other surface proteins in adhesion to milk proteins in absence of SpaCBA pili. To study the role of others LGG surface biomolecules (*i.e.* other than SpaCBA pili), two LGG mutants depleted in SpaCBA pili are compared: LGG *spaCBA* and LGG *welEspaCBA*. LGG *spaCBA* surface is composed of a long rich-galactose EPS layer, small glucose-rich EPS and proteins as MBF or MabA (**Figure 5A**) (Francius et al., 2009; Perea Vélez et al., 2010; von Ossowski et al., 2011). The percentages of adhesive events between LGG *spaCBA* and the different milk proteins are of 13.5 ± 5.5, 13.5 ± 0.5 and 11.0 ± 3.0 % for β-LG, α-LA and BSA, respectively (**Figure 5B**) and are not significantly different from each other. First, results observed with β-LG demonstrated a dramatic decrease of adhesive events in absence of SpaCBA pili on LGG surface, which reinforce the key role of pili in adhesion between LGG and β-LG. In contrast, specific biomolecules stretching signatures recorded on retraction curves are rare but highly reproducible for all whey proteins (**Figure 5C, D, E**). The rupture number is ranging from 1 and 2, the maximal force varies between 100 and 200 pN and the maximal stretching distance is ranging from 0.6 and 1.4 µm. These signatures are similar to those observed by Francius *et al.* (2009) when they used lectin-functionalized AFM tips. Francius *et al.* (2009) obtained the same multiple force peak with a magnitude ranging from 50 to 100 pN and up to 1000 nm length during the stretching of EPS. In another work, similar results are obtained during the LGG *spaCBA* adhesion to hydrophobic surfaces. The observed forces profiles resemble to those obtained from stretching of EPS on LGG cells (Sullan et al., 2014). Signatures recorded with LGG *spaCBA* during biomolecules stretching seem to be those of sugars which should correspond to the stretching behavior of EPS (Francius et al., 2009). Thus, in the absence of SpaCBA pilus, all whey proteins may be able to interact with LGG via EPS. With the casein-modified tip, interaction with bacterial surface reveals specific

signatures of biomolecules stretching (**Figure 5F**). The rupture number is of 2.8 ± 0.2, the maximal force is of 1.8 ± 0.1 pN and the maximal stretching distance is of 1.1 ± 0.1 µm (**Figure 5F**). With caseins, the particular shape of the retraction curves does not allow the determination of the biomolecule involved in the interaction with LGG SpaCBA.

In conclusion, these results demonstrated the ability of EPS to interact with milk proteins, in a less pronounced way than pili and only when pili are absent. These results suppose that the presence of pili masked the other biomolecules and inhibit their ability to mediate adhesion to milk proteins.

The surface of LGG *welEspaCBA* mutant is composed of different biomolecules such as small glucose-rich EPS, other proteins as MBF or MabA, lipoteichoïc acids or peptidoglycans (**Figure 6A**) (Lebeer et al., 2012). The percentages of adhesive events measured with LGG *welEspaCBA* are of 44.0 ± 6.7, 17.5 ± 0.5 and 14.0 ± 2.0 % for β-LG, α-LA and BSA, respectively (**Figure 6B**). No specific adhesive events are observed between LGG *welEspaCBA* and caseins. The specific signatures recorded for whey proteins on retraction curves are presented on **Figures 6C, D and E**. These specific signatures revealed the presence of surface biomolecules, other than SpaCBA pili and long EPS, implicated in adhesion with whey proteins. The observed signatures may recall the small EPS stretching (Francius et al., 2009). These signatures may also be due to the detection of peptidoglycan, accessible in the absence of both long-EPS and SpaCBA pili, with the milk proteins (Beaussart et al., 2013) and the observed peak will be due to the stretching of milk proteins. Nevertheless, other surface mutants will be required to validate these hypotheses.

Conclusion

AFM in force mode was used in this work to underline the role of LGG surface biomolecules in adhesion to milk proteins. The high frequency of adhesive events demonstrated that the SpaCBA pili and other LGG surface biomolecules such as EPS and proteins are involved in the adhesion. However, the ability of each biomolecule to interact with milk proteins depend on their environment. In LGG WT, only the pili are implicated in adhesive interactions with the β-LG as other surface biomolecules are masked. When pili are absents, the results demonstrated that EPS are also able to interact with all milk proteins, in a less pronounced way than pili. This work revealed the ability of LGG surface biomolecules to interact to different milk proteins. Depending on the surface biomolecules composition, LAB present different affinity with milk components. In that respect, it is expected that the media and the growth phase may have an impact on the preferential location of bacteria in the dairy matrix, and could be extended to other LAB strains.

Acknowledgement

The authors thank the Centre of Microbial and Plant Genetics, KU Leuven and the Department of Bioscience Engineering, University of Antwerp for providing the bacterial strains.

References

Beaussart, A., Rolain, T., Duchêne, M.-C., El-Kirat-Chatel, S., Andre, G., Hols, P., & Dufrêne, Y. F. (2013). Binding Mechanism of the Peptidoglycan Hydrolase Acm2: Low Affinity, Broad Specificity. *Biophysical Journal*, *105*(3), 620–629. https://doi.org/10.1016/j.bpj.2013.06.035

Burgain, J., Gaiani, C., Francius, G., Revol-Junelles, A. M., Cailliez-Grimal, C., Lebeer, S., … Scher, J. (2013). In vitro interactions between probiotic bacteria and milk proteins probed by atomic force microscopy. *Colloids and Surfaces. B, Biointerfaces*, *104*, 153–162. https://doi.org/10.1016/j.colsurfb.2012.11.032

Burgain, J., Scher, J., Lebeer, S., Vanderleyden, J., Corgneau, M., Guerin, J., … Gaiani, C. (2015). Impacts of pH-mediated EPS structure on probiotic bacterial pili–whey proteins interactions. *Colloids and Surfaces B: Biointerfaces*, *134*, 332–338. https://doi.org/10.1016/j.colsurfb.2015.06.068

Çelebioğlu, H. Y., Gudjónsdóttir, M., Meier, S., Duus, J. Ø., Lee, S., & Chronakis, I. S. (2015). Spectroscopic studies of the interactions between β-lactoglobulin and bovine submaxillary mucin. *Food Hydrocolloids*, *50*, 203–210. https://doi.org/10.1016/j.foodhyd.2015.04.026

Dominguez-Ramirez, L., Del Moral-Ramirez, E., Cortes-Hernandez, P., Garcia-Garibay, M., & Jimenez-Guzman, J. (2013). beta-lactoglobulin's conformational requirements for ligand binding at the calyx and the dimer interphase: a flexible docking study. *PLoS One*, *8*(11), e79530. https://doi.org/10.1371/journal.pone.0079530

Fox, P. F. (2008). Milk: an overview. In A. Thompson, M. Boland, & H. Singh (Eds.), *Milk Proteins* (pp. 1–54). San Diego: Academic Press. https://doi.org/10.1016/B978-0-12-374039-7.00001-5

Francius, G., Alsteens, D., Dupres, V., Lebeer, S., De Keersmaecker, S., Vanderleyden, J., … Dufrêne, Y. F. (2009). Stretching polysaccharides on live cells using single molecule force spectroscopy. *Nature Protocols*, *4*(6), 939–946. https://doi.org/10.1038/nprot.2009.65

Guerin, J., Bacharouche, J., Burgain, J., Lebeer, S., Francius, G., Borges, F., … Gaiani, C. (2016). Pili of Lactobacillus rhamnosus GG mediate interaction with β-lactoglobulin. *Food Hydrocolloids*, *58*, 35–41. https://doi.org/10.1016/j.foodhyd.2016.02.016

Hickey, C. D., Auty, M. A. E., Wilkinson, M. G., & Sheehan, J. J. (2015). The influence of cheese manufacture parameters on cheese microstructure, microbial localisation and their interactions during ripening: A review. *Trends in Food Science & Technology*, *41*(2), 135–148. https://doi.org/10.1016/j.tifs.2014.10.006

Hickey, C. D., Sheehan, J. J., Wilkinson, M. G., & Auty, M. A. E. (2015). Growth and location of bacterial colonies within dairy foods using microscopy techniques: a review. *Food Microbiology*, *6*, 99. https://doi.org/10.3389/fmicb.2015.00099

Kankainen, M., Paulin, L., Tynkkynen, S., von Ossowski, I., Reunanen, J., Partanen, P., … de Vos, W. M. (2009). Comparative genomic analysis of Lactobacillus rhamnosus GG reveals pili containing a human- mucus binding protein. *Proc Natl Acad Sci U S A*, *106*(40), 17193–17198. https://doi.org/10.1073/pnas.0908876106

Kontopidis, G., Holt, C., & Sawyer, L. (2002). The ligand-binding site of bovine beta-lactoglobulin: evidence for a function? *J Mol Biol*, *318*(4), 1043–1055. https://doi.org/10.1016/s0022-2836(02)00017-7

Kontopidis, G., Holt, C., & Sawyer, L. (2004). Invited Review: β-Lactoglobulin: Binding Properties, Structure, and Function. *Journal of Dairy Science*, *87*(4), 785–796. https://doi.org/10.3168/jds.S0022-0302(04)73222-1

Laloy, E., Vuillemard, J.-C., El Soda, M., & Simard, R. E. (1996). Influence of the fat content of Cheddar cheese on retention and localization of starters. *International Dairy Journal*, *6*(7), 729–740. https://doi.org/10.1016/0958-6946(95)00068-2

Lebeer, S., Claes, I. J. J., Verhoeven, T. L. A., Vanderleyden, J., & De Keersmaecker, S. C. J. (2011). Exopolysaccharides of Lactobacillus rhamnosus GG form a protective shield against innate immune factors in the intestine. *Microbial Biotechnology*, *4*(3), 368–374. https://doi.org/10.1111/j.1751-7915.2010.00199.x

Lebeer, S., Claes, I., Tytgat, H. L., Verhoeven, T. L., Marien, E., von Ossowski, I., … Vanderleyden, J. (2012). Functional analysis of Lactobacillus rhamnosus GG pili in relation to adhesion and immunomodulatory interactions with intestinal epithelial cells. *Appl Environ Microbiol*, *78*(1), 185–193. https://doi.org/10.1128/aem.06192-11

Lebeer, S., Verhoeven, T. L., Francius, G., Schoofs, G., Lambrichts, I., Dufrene, Y., … De Keersmaecker, S. C. (2009). Identification of a gene cluster for the biosynthesis of a long galactose-rich exopolysaccharide in Lactobacillus rhamnosus GG and functional analysis of the priming glycosyltransferase. *Appl Environ Microbiol*, *75*, 3554–3563. https://doi.org/10.1128/AEM.02919-08

Leroy, F., & De Vuyst, L. (2004). Lactic acid bacteria as functional starter cultures for the food fermentation industry. *Trends in Food Science & Technology*, *15*(2), 67–78. https://doi.org/10.1016/j.tifs.2003.09.004

Linares, D. M., Ross, P., & Stanton, C. (2016). Beneficial Microbes: The pharmacy in the gut: Bioengineered: Vol 7, No 1. *Bioengineered*, *7*, 11–20.

Lopez, C., Maillard, M.-B., Briard-Bion, V., Camier, B., & Hannon, J. A. (2006). Lipolysis during ripening of Emmental cheese considering organization of fat and preferential localization of bacteria. *Journal of Agricultural and Food Chemistry*, *54*(16), 5855–5867. https://doi.org/10.1021/jf060214l

Monaco, H. L., Zanotti, G., Spadon, P., Bolognesi, M., Sawyer, L., & Eliopoulos, E. E. (1987). Crystal structure of the trigonal form of bovine beta-lactoglobulin and of its complex with retinol at 2.5 A resolution. *J Mol Biol*, *197*(4), 695–706.

Oberg, C., McManus, W., & McMahon, D. (1993). Microstructure of Mozzarella Cheese During Manufacture. *Food Structure*, *12*(2). Retrieved from http://digitalcommons.usu.edu/foodmicrostructure/vol12/iss2/12

Perea Vélez, M., Petrova, M. I., Lebeer, S., Verhoeven, T. L. A., Claes, I., Lambrichts, I., … De Keersmaecker, S. C. J. (2010). Characterization of MabA, a modulator of Lactobacillus rhamnosus GG adhesion and biofilm formation. *FEMS Immunology & Medical Microbiology*, *59*(3), 386–398. https://doi.org/10.1111/j.1574-695X.2010.00680.x

Reunanen, J., von Ossowski, I., Hendrickx, A. P., Palva, A., & de Vos, W. M. (2012). Characterization of the SpaCBA pilus fibers in the probiotic Lactobacillus rhamnosus GG. *Appl Environ Microbiol*, *78*(7), 2337–2344. https://doi.org/10.1128/aem.07047-11

Salotti de Souza, B. M., Borgonovi, T. F., Casarotti, S. N., Todorov, S. D., & Penna, A. L. B. (2018). Lactobacillus casei and Lactobacillus fermentum Strains Isolated from Mozzarella Cheese: Probiotic Potential, Safety, Acidifying Kinetic Parameters and Viability under Gastrointestinal Tract Conditions. *Probiotics and Antimicrobial Proteins*. https://doi.org/10.1007/s12602-018-9406-y

Sullan, R. M. A., Beaussart, A., Tripathi, P., Derclaye, S., El-Kirat-Chatel, S., Li, J. K., … Dufrene, Y. F. (2014). Single-cell force spectroscopy of pili-mediated adhesion. *Nanoscale*, *6*(2), 1134–1143. https://doi.org/10.1039/c3nr05462d

Tripathi, P., Beaussart, A., Alsteens, D., Dupres, V., Claes, I., von Ossowski, I., … Dufrene, Y. F. (2013). Adhesion and Nanomechanics of Pili from the Probiotic Lactobacillus rhamnosus GG. *ACS Nano*, *7*(4), 3685–3697. https://doi.org/10.1021/nn400705u

Tripathi, P., Dupres, V., Beaussart, A., Lebeer, S., Claes, I. J. J., Vanderleyden, J., & Dufrene, Y. F. (2012). Deciphering the Nanometer-Scale Organization and Assembly of Lactobacillus rhamnosus GG Pili Using Atomic Force Microscopy. *Langmuir*, *28*(4), 2211–2216. https://doi.org/10.1021/la203834d

Tunick, M. H., Mackey, K. L., Shieh, J. J., Smith, P. W., Cooke, P., & Malin, E. L. (1993). Rheology and microstructure of low-fat Mozzarella cheese. *International Dairy Journal*, *3*(7), 649–662. https://doi.org/10.1016/0958-6946(93)90106-A

Tytgat, H. L. P., van Teijlingen, N. H., Sullan, R. M. A., Douillard, F. P., Rasinkangas, P., Messing, M., … Lebeer, S. (2016). Probiotic Gut Microbiota Isolate Interacts with Dendritic Cells via Glycosylated Heterotrimeric Pili. *PloS One*, *11*(3), e0151824. https://doi.org/10.1371/journal.pone.0151824

von Ossowski, I., Satokari, R., Reunanen, J., Lebeer, S., De Keersmaecker, S. C. J., Vanderleyden, J., … Palva, A. (2011). Functional characterization of a mucus-specific LPXTG surface adhesin from probiotic Lactobacillus rhamnosus GG. *Applied and Environmental Microbiology*, *77*(13), 4465–4472. https://doi.org/10.1128/AEM.02497-10

Figure 1

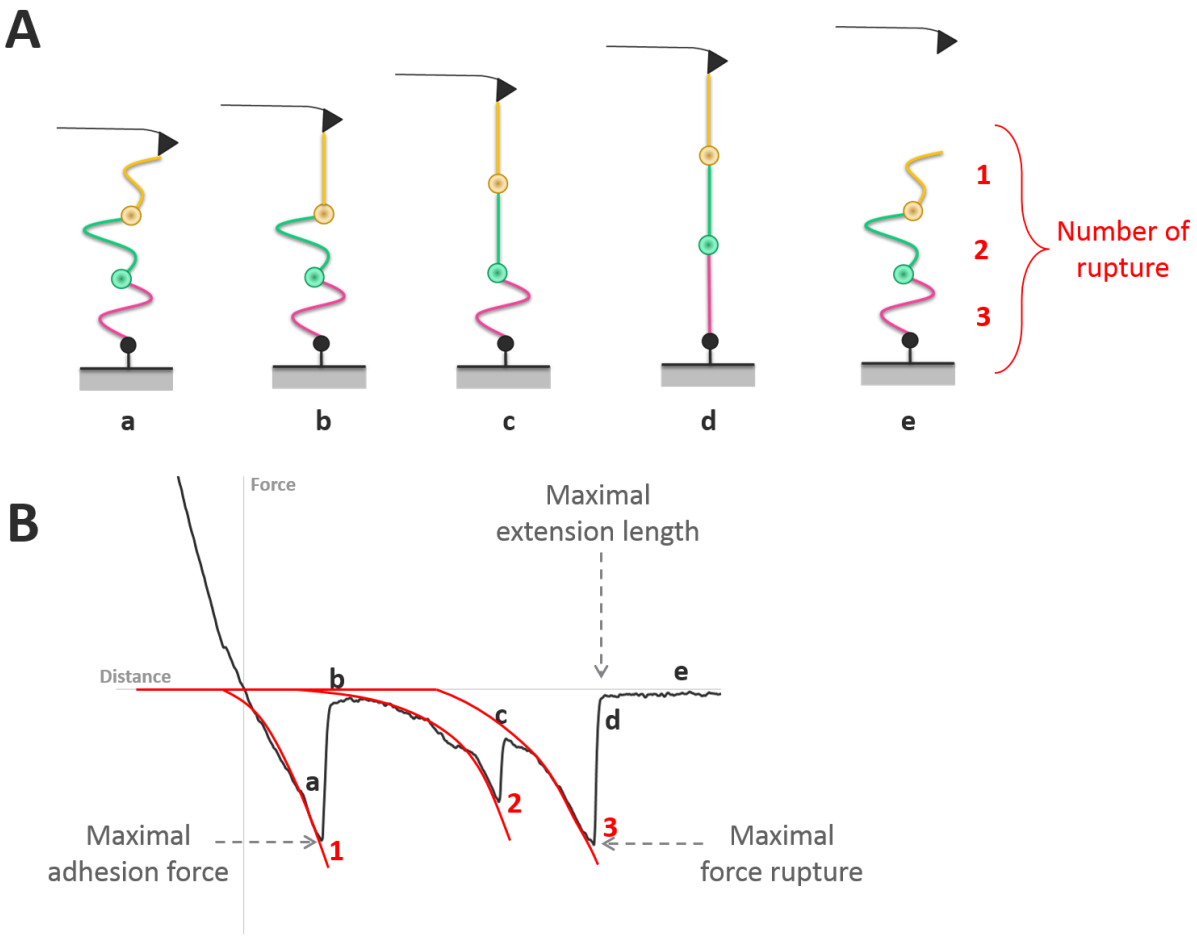
A
a
b
c
d
e
1
2
3
Number of rupture
B
Force
Distance
Maximal extension length
Maximal adhesion force
Maximal force rupture

Figure 2

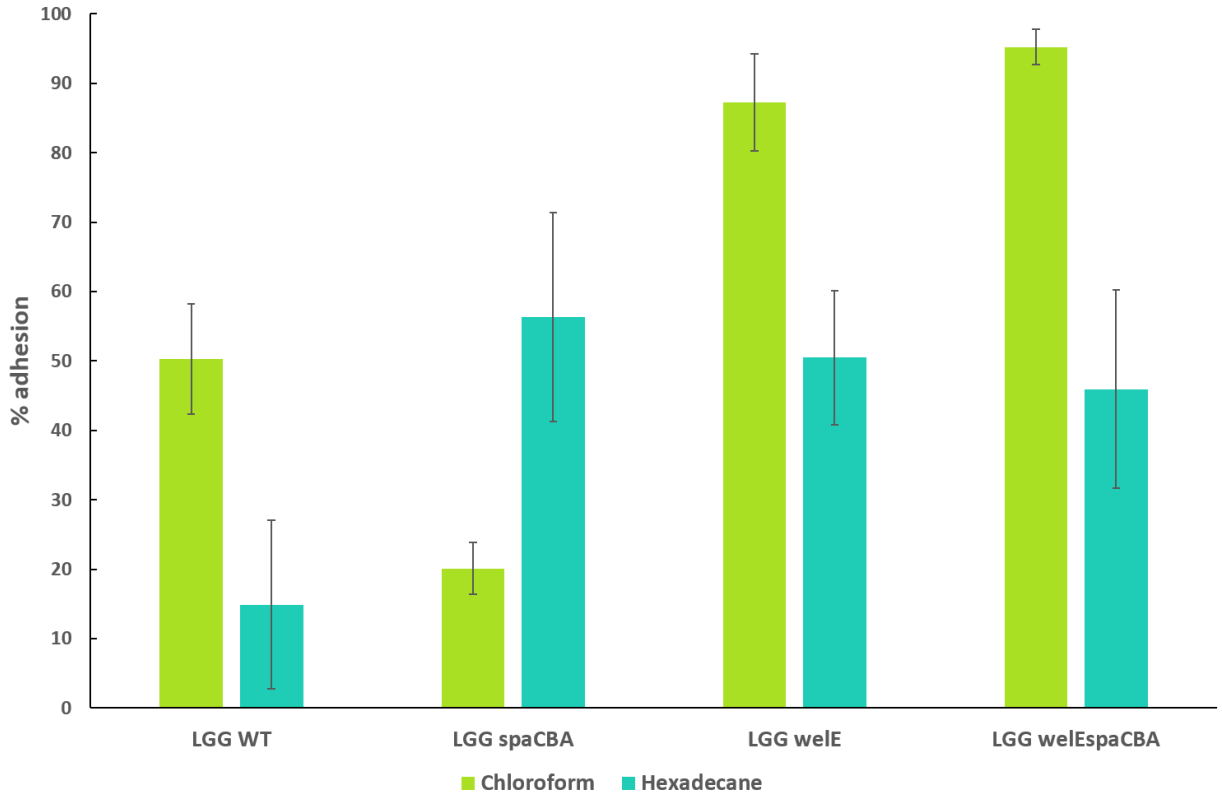
100
90
80
70
60
50
40
30
20
10
0
% adhesion
LGG WT
LGG spaCBA
LGG welE
LGG welEspaCBA
Chloroform
Hexadecane

Figure 3

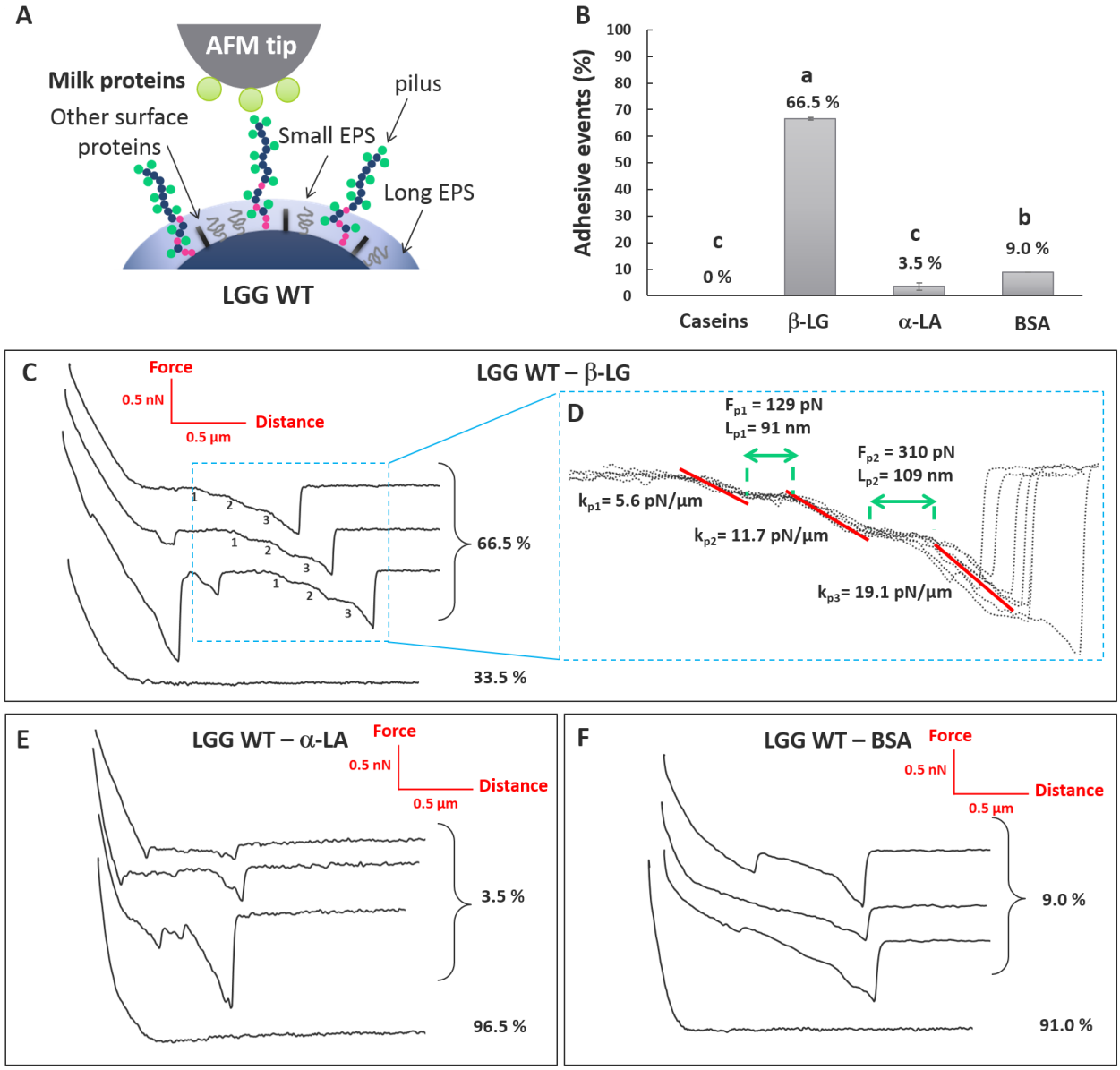
A
AFM tip
Milk proteins
Other surface proteins
pilus
Small EPS
Long EPS
LGG WT
B
Adhesive events (%)
a
66.5 %
c
0 %
c
3.5 %
b
9.0 %
Caseins
β-LG
α-LA
BSA
C
Force
0.5 nN
Distance
0.5 µm
LGG WT – β-LG
66.5 %
33.5 %
D
Fp1 = 129 pN
Lp1= 91 nm
Fp2 = 310 pN
Lp2= 109 nm
kp1= 5.6 pN/µm
kp2= 11.7 pN/µm
kp3= 19.1 pN/µm
E
LGG WT – α-LA
3.5 %
96.5 %
F
LGG WT – BSA
9.0 %
91.0 %

449 **Figure 4**

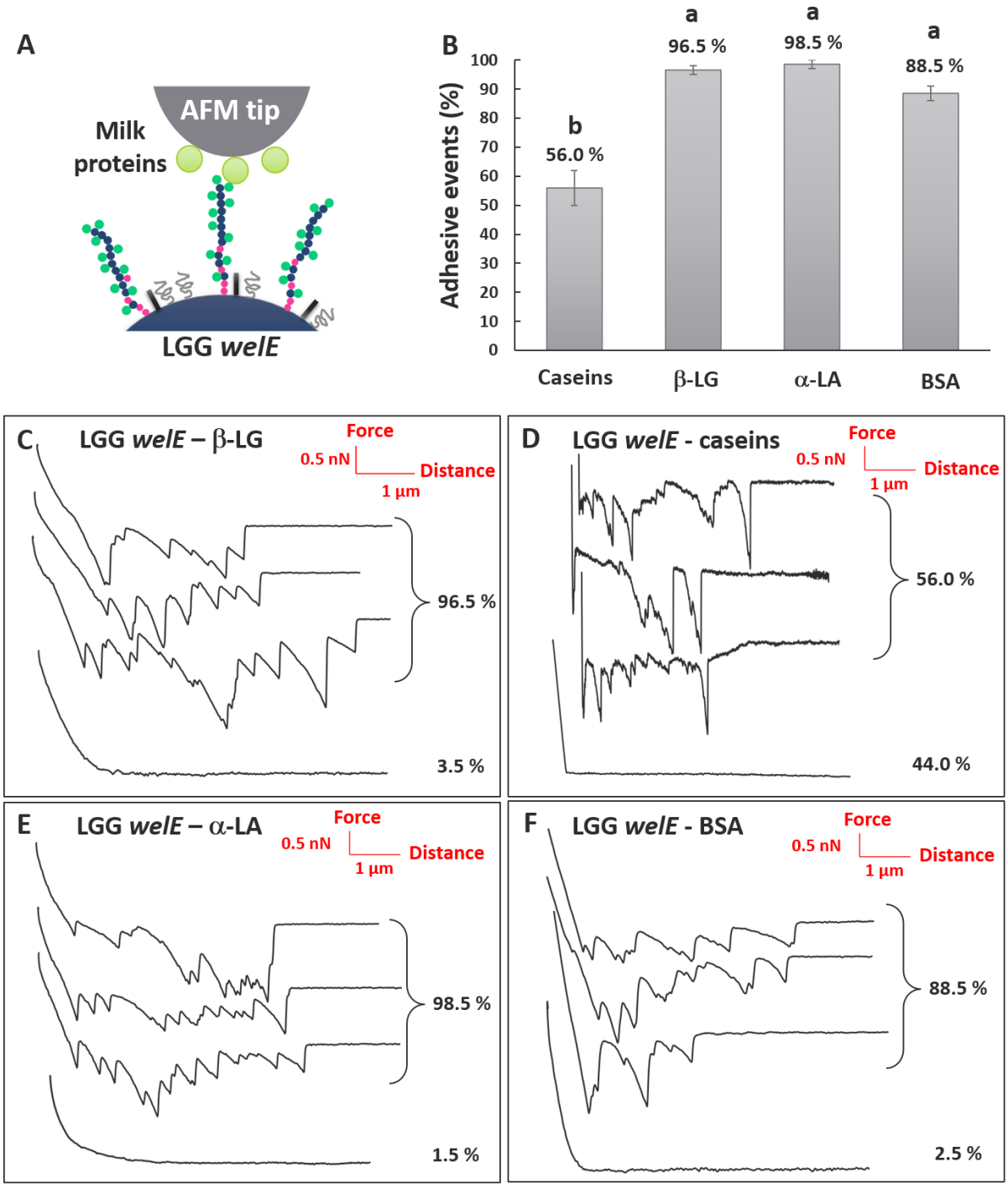

450

451

Figure 5

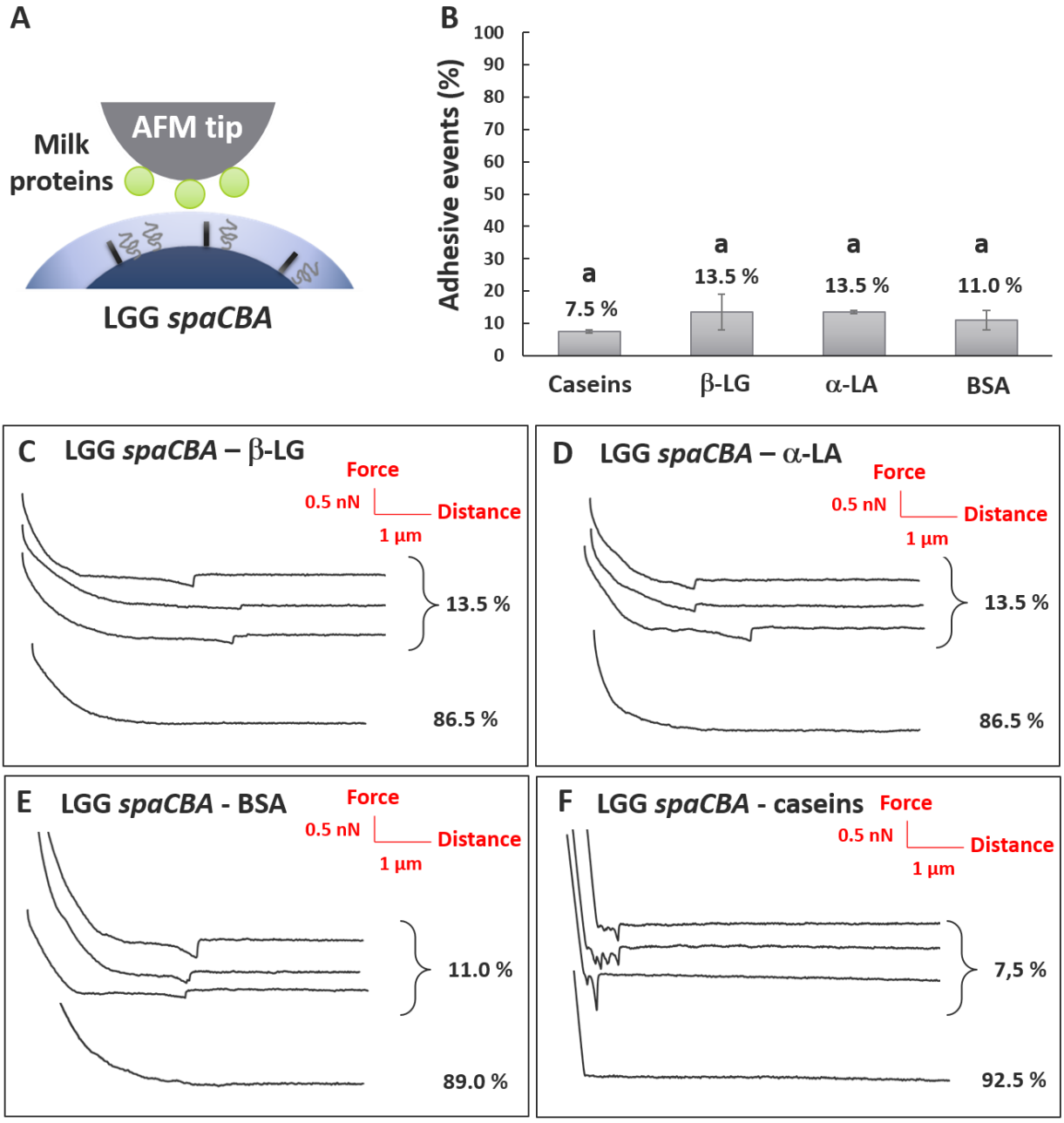
A
AFM tip
Milk proteins
LGG spaCBA
B
Adhesive events (%)
100
90
80
70
60
50
40
30
20
10
0
a
7.5 %
a
13.5 %
a
13.5 %
a
11.0 %
Caseins
β-LG
α-LA
BSA
C LGG spaCBA – β-LG
Force
0.5 nN
Distance
1 µm
13.5 %
86.5 %
D LGG spaCBA – α-LA
Force
0.5 nN
Distance
1 µm
13.5 %
86.5 %
E LGG spaCBA - BSA
Force
0.5 nN
Distance
1 µm
11.0 %
89.0 %
F LGG spaCBA - caseins
Force
0.5 nN
Distance
1 µm
7,5 %
92.5 %

Figure 6

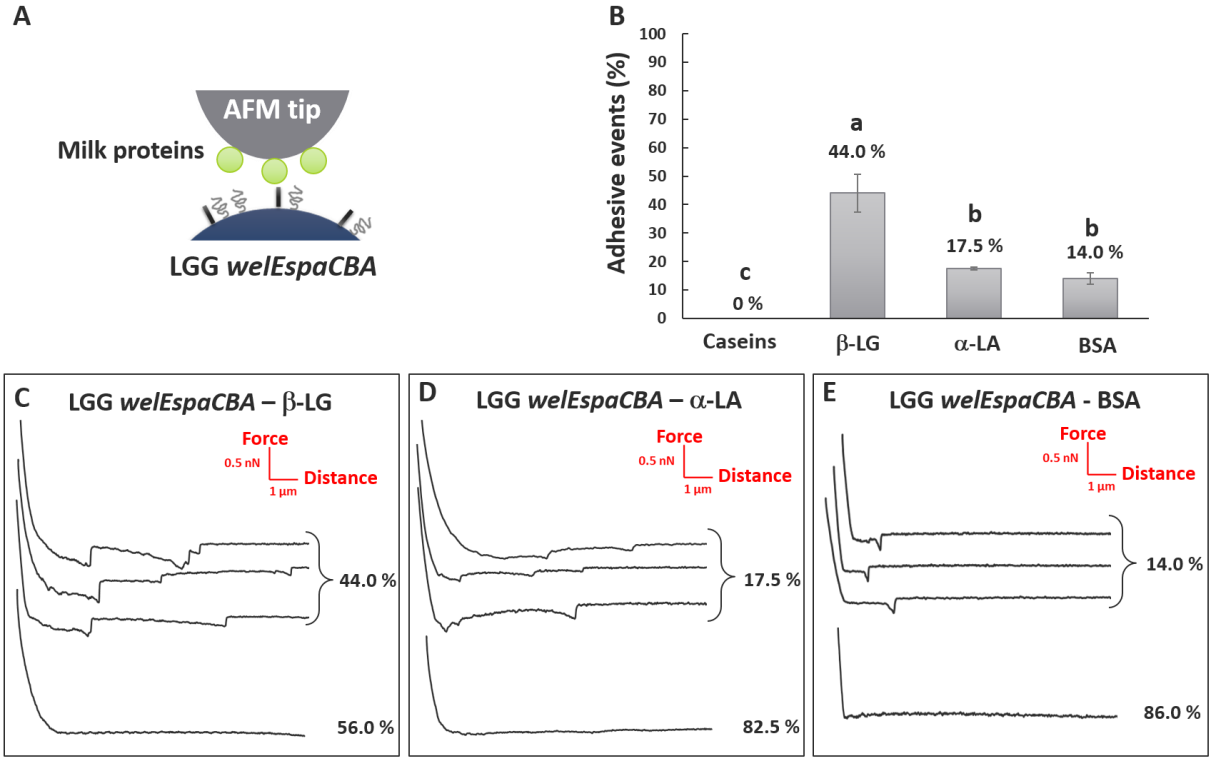
A
AFM tip
Milk proteins
LGG welEspaCBA
B
Adhesive events (%)
100
90
80
70
60
50
40
30
20
10
0
a
44.0 %
b
17.5 %
b
14.0 %
c
0 %
Caseins
β-LG
α-LA
BSA
C
LGG welEspaCBA – β-LG
Force
0.5 nN
Distance
1 µm
44.0 %
56.0 %
D
LGG welEspaCBA – α-LA
Force
0.5 nN
Distance
1 µm
17.5 %
82.5 %
E
LGG welEspaCBA - BSA
Force
0.5 nN
Distance
1 µm
14.0 %
86.0 %

Figure captions

Figure 1: Illustration of a biomolecule displaying force-induced structural modification (A). Example of data obtained by adjustment of the retraction curve with the FJC or WLC models (red lines) (B).

Figure 2: Microbial adhesion to solvents test to determine the surface hydrophobicity of LGG WT and the three mutants: LGG *spaCBA*, LGG *welE* and LGG *welEspaCBA*.

Figure 3: Adhesive interactions between LGG WT and milk proteins (caseins, β-LG, α-LA and BSA).

Schema of the principle of AFM-based force spectroscopy to measure the interaction between milk proteins coated probes and the surface of LGG WT (A). Frequency of adhesive events between LGG and individual milk proteins (B). Representative retraction curves recorded between LGG and β-LG (C). Superimposition of retraction curves and determination of spring-like properties of pili SpaCBA (D). Representative retraction curves recorded between LGG and α-LA (E) or BSA (F).

Figure 4: Adhesion between LGG *welE* and milk proteins.

Schema of the principle of AFM-based force spectroscopy to measure the interaction between milk proteins coated probes and the surface of LGG welE (A). Frequency of adhesive events between LGG and individual milk proteins (B). Representative retraction curves recorded between LGG and β-LG (C), caseins (D), α-LA (E) or BSA (F).

Figure 5: Adhesion between LGG *spaCBA* and milk proteins.

Schema of the principle of AFM-based force spectroscopy to measure the interaction between milk proteins coated probes and the surface of LGG spaCBA (A). Frequency of adhesive events between LGG and individual milk proteins (B). Representative retraction curves recorded between LGG and β-LG (C), α-LA (D), BSA (E) or caseins (F).

Figure 6: Adhesion between LGG *welEspaCBA* and milk proteins.

Schema of the principle of AFM-based force spectroscopy to measure the interaction between milk proteins coated probes and the surface of LGG welEspaCBA (A). Frequency of adhesive events

between LGG and individual milk proteins (B). Representative retraction curves recorded between LGG and β-LG (C), α-LA (D) or BSA (E).